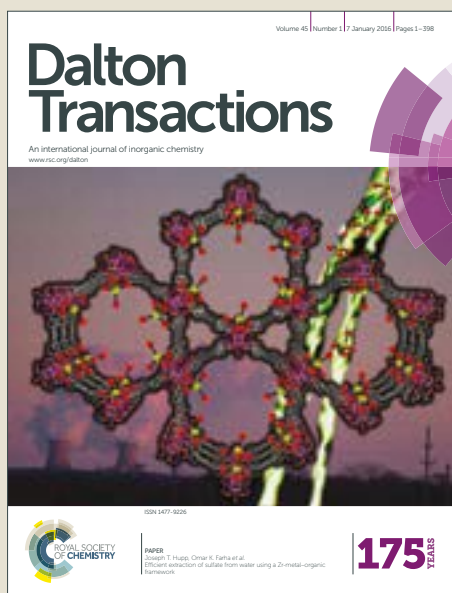


Dalton Transactions

Accepted Manuscript



This article can be cited before page numbers have been issued, to do this please use: R. Karmis, S. Carrara, A. Baxter, C. F. Hogan, M. Hulett and P. Barnard, *Dalton Trans.*, 2019, DOI: 10.1039/C9DT01362H.



This is an Accepted Manuscript, which has been through the Royal Society of Chemistry peer review process and has been accepted for publication.

Accepted Manuscripts are published online shortly after acceptance, before technical editing, formatting and proof reading. Using this free service, authors can make their results available to the community, in citable form, before we publish the edited article. We will replace this Accepted Manuscript with the edited and formatted Advance Article as soon as it is available.

You can find more information about Accepted Manuscripts in the [author guidelines](#).

Please note that technical editing may introduce minor changes to the text and/or graphics, which may alter content. The journal's standard [Terms & Conditions](#) and the ethical guidelines, outlined in our [author and reviewer resource centre](#), still apply. In no event shall the Royal Society of Chemistry be held responsible for any errors or omissions in this Accepted Manuscript or any consequences arising from the use of any information it contains.

Luminescent Iridium(III) Complexes of N-Heterocyclic Carbene Ligands Prepared Using the 'Click Reaction'

View Article Online
DOI: 10.1039/C9DT01362H

Rebecca E. Karmis,^a Serena Carrara,^a Amy A. Baxter,^b Conor F. Hogan,^a Mark D. Hulett^b and Peter J. Barnard^{a*}

^a*Department of Chemistry and Physics, La Trobe Institute for Molecular Science, La Trobe University, Victoria, 3086, Australia, Fax: (+)61 3 9479 1266, E-mail: p.barnard@latrobe.edu.au*

^b*Department of Biochemistry and Genetics, La Trobe Institute for Molecular Science, La Trobe University, Victoria, 3086, Australia.*

Abstract

A series of imidazolium salt, N-heterocyclic carbene (NHC) ligand precursors, combined with 1,2,3-triazoles were synthesized using the Cu(I) catalyzed azide-alkyne cycloaddition 'click reaction'. These pro-ligands were prepared from imidazolium molecules that were functionalized with either a terminal alkyne or azide groups. Methylation of the triazole unit with methyl iodide produced a series of imidazolium / triazolium NHC pro-ligands. From these pro-ligands a family of luminescent Ir(III) complexes of the general form $[\text{Irppy})_2(\text{C}^{\wedge}\text{N})]^+$ or $[\text{Ir(ppy)}_2(\text{C}^{\wedge}\text{C})]^+$ (where ppy is 2-phenylpyridine and $\text{C}^{\wedge}\text{N}$ represents a bidentate imidazolylidene/triazole ligand and $\text{C}^{\wedge}\text{C}$ represents a bidentate imidazolylidene / triazolylidene ligand) were prepared. The electrochemical, photophysical and electrochemiluminescence properties of the complexes have been evaluated and a preliminary of two of these compounds as luminescent probes for cell imaging studies was conducted in A549 human lung adenocarcinoma basal epithelial cells. Co-localisation studies with the commercial dye Mitotracker CMXRos were consistent with mitochondrial uptake for these compounds.

Introduction

N-heterocyclic carbene (NHC) ligands are well known for their synthetic versatility and impressive electron donating properties¹ and metal complexes of NHCs have been evaluated for a variety of applications, including homogeneous catalysis,²⁻⁶ electroluminescent materials for the development of organic light emitting diodes (OLEDs),^{7,8} and for a variety of biological applications such as antimicrobial and anticancer agents.^{9, 10} The versatility of NHCs is illustrated by the incorporation of the naphthalimide chromophore into a series of NHC ligands to provide deep-red to NIR emitting Ir(III) complexes.^{11, 12} Some ten years after the first isolation of a free imidazolylidene

by Arduengo in 1991,¹³ experimental and computational studies have shown that NHCs can behave as carbenes not only at the ‘normal’ C-2 position but also at the ‘abnormal’ C-4 position.^{14, 15} In this series of studies, ‘abnormal’ or mesoionic C-4 coordination was found to occur in preference to the ‘normal’ NHC binding mode for steric and kinetic reasons.^{14, 16} Later, in 2009 Bertrand isolated and characterized the first example of an ‘abnormal’ imidazole-based carbene.¹⁷

Since Sharpless and co-workers reported the Cu(I) azide-alkyne cycloaddition reaction (CuAAC) or the ‘click reaction’, 1,2,3-triazoles and the mesoionic carbenes derived from these species (1,2,3-triazolylidenes) are now well established as efficient donors for a range of metals.¹⁸⁻³¹ The 1,2,3-triazole moiety can coordinate to metals via either the N2 or N3 positions and experimental observations in combination with DFT studies have shown coordination via the N3 position tends to result in stronger metal-ligand binding.^{32, 33} The combination of 1,2,3-triazole donors with imidazole-based NHCs has been previously examined^{34, 35} and Rh(I), Rh(III) and Ir(III) complexes with this ligand system (e.g. **I** Figure 1) were evaluated as catalysts for the intramolecular hydroamination of aminoalkynes.³⁶ Mixed imidazolium/1,2,3-triazolium pro-ligand have been used to prepare mononuclear dicarbene complexes (e.g. **II** Figure 1) and asymmetrical mixed-metal complexes.^{37, 38}

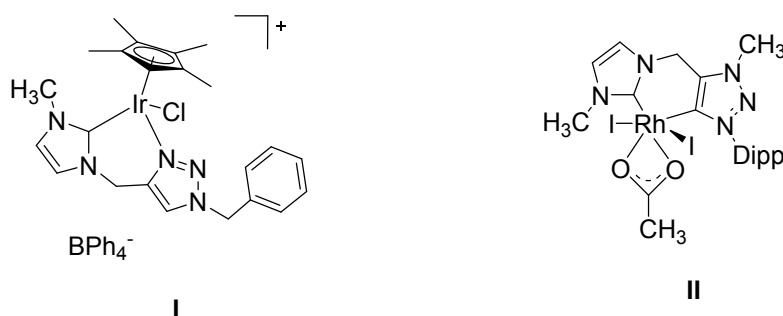


Figure 1. **I** Ir(I) complex of a bidentate NHC / 1,2,3-triazole ligand and **II** a Rh(III) complex of a bidentate imidazolylidene / triazolylidene ligand.

Attractive features often associated with luminescent Ir(III) complexes, such as large Stokes shifts, high photostability and long excited state lifetimes have led to them being explored as probes for cell imaging studies and the cellular distribution of a range of complexes has been previously evaluated.³⁹⁻⁴² Significantly, specific organellular uptake, including lysosomal⁴³, mitochondrial⁴⁴⁻⁵⁰ and phospholipid membrane⁵¹ labeling has been reported and in a highly pertinent study, a luminescent Ir(III) complexes of biscarbene ligands were shown to specifically stain the endoplasmic reticulum.⁵²

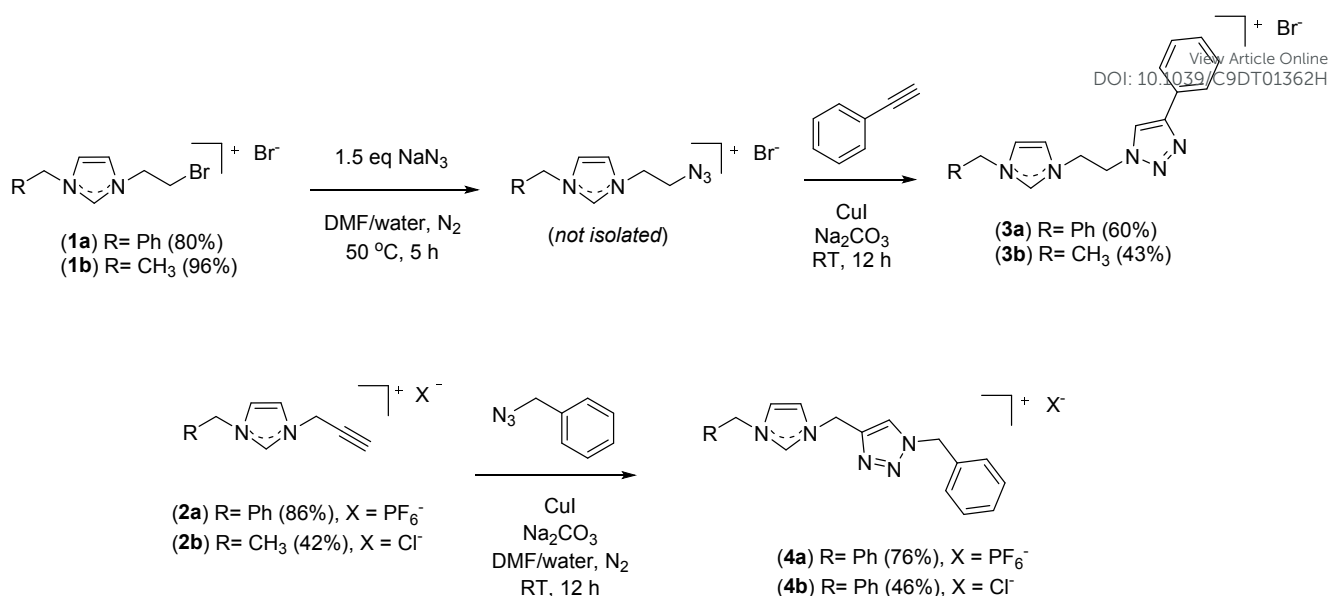
We have a long-standing interest in the synthesis and evaluation of new luminescent complexes of NHC ligands and have previously reported luminescent NHC complexes of the metals Ru,⁵³ Ir,⁵⁴⁻⁵⁶ Re^{57, 58} and Au.^{59, 60} In the present paper, the use of a one-pot ‘click reaction’ for the synthesis of a series of four pro-ligands that combine imidazolium units with 1,2,3 triazoles is

described. Utilizing these compounds, a second set of pro-ligands combining imidazolium and 1,2,3-triazolium groups were prepared by methylation of the chosen 1,2,3-triazole with iodomethane. From these pro-ligands, a series of five heteroleptic Ir(III) complexes of the general form $[\text{Ir}(\text{ppy})_2(\text{N}^{\wedge}\text{C})]^+$ $[\text{Ir}(\text{ppy})_2(\text{C}^{\wedge}\text{C})]^+$ were prepared (where ppy represents 2-phenylpyridine and $\text{N}^{\wedge}\text{C}$ represents a bidentate triazole substituted imidazolylidene ligand and $\text{C}^{\wedge}\text{C}$ represents a 1,2,3-triazolylidene / imidazolylidene ligand). The complexes are luminescent and their photophysical and electrochemical and electrochemiluminescent properties were evaluated. Finally, due to the synthetic versatility of these ligand systems, a preliminary evaluation of the use of these compounds as luminescent probes for cell imaging studies was conducted.

Results and Discussion

Ligand Synthesis

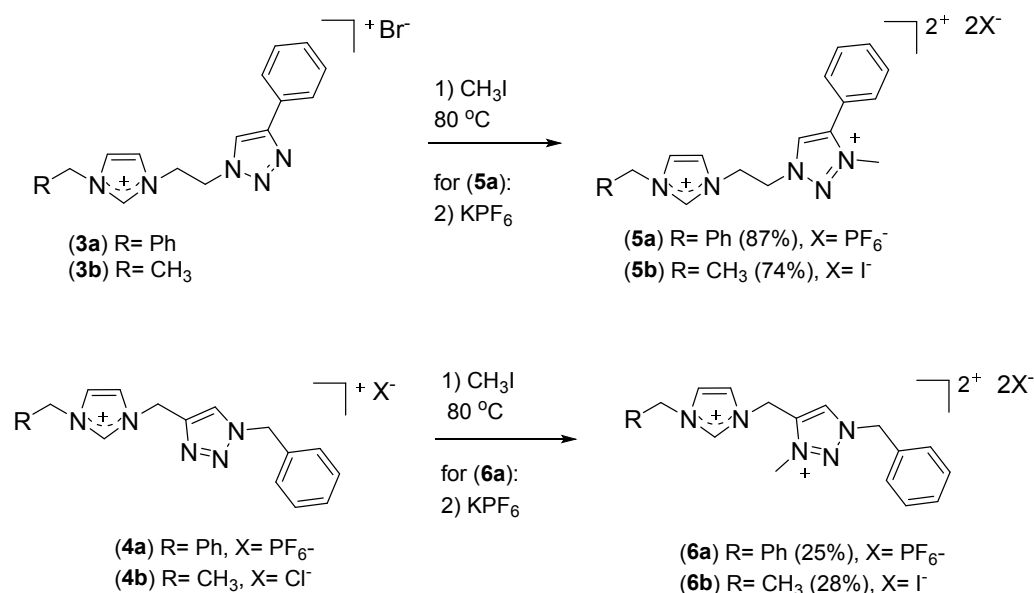
Two classes of imidazolium salt, N-heterocyclic carbene pro-ligands linked to 1,2,3-triazole units were prepared and their structures are shown in Scheme 1 (class **I** = **3a**, **3b** and class **II** = **4a**, **4b**). The preparation of ligands **3a** and **3b** involved the initial synthesis of an azide substituted azolium salt. Due to safety concerns associated with the isolation of organic azides a one-pot synthetic procedure was developed for the formation of the 1,2,3-triazole unit. In this procedure, the required azide was generated *in situ* by the reaction of a 2-bromoethyl functionalized imidazolium salt precursor (**1a** and **1b**) with sodium azide. These synthetic reactions were monitored by TLC and upon completion, the components for triazole formation (phenylacetylene, CuI, and the base Na_2CO_3) were added to the mixture.¹⁸ Initially, attempts were made to carry out the 'click reactions' using a Cu(II) salt (e.g. CuSO_4 or $\text{Cu}(\text{CH}_3\text{CO}_2)_2$) in the presence of the reducing agent ascorbic acid to generate the Cu(I) catalyst *in situ*.^{18, 27, 61} This approach was unsuccessful as the cationic imidazolium salts formed could not be isolated from the reaction mixtures. To allow for a simpler workup, the reactions were instead conducted using CuI as the catalyst under an atmosphere of N_2 to avoid oxidation of the cuprous ion. Using this approach, the Cu(I) salts could be readily removed at the end of the reaction by filtration.



Scheme 1. (Upper panel) Synthesis of class **I** pro-ligands **3a** and **3b** (the azide functionalized imidazolium salts were prepared *in situ*) and (lower panel) synthesis of class **II** pro-ligands **4a** and **4b**.

The second class of pro-ligands (class **II**, **4a** and **4b**, Scheme 1) were prepared from the propargyl functionalized imidazolium salts (**2a** and **2b**), which were synthesized by the alkylation of either 1-phenyl- or 1-ethyl-imidazole with propargyl *p*-toluenesulfonate. The 1,2,3-triazole functionalized pro-ligands were then synthesized from **2a** or **2b** and benzyl azide, using the same azide-alkyne cycloaddition conditions that were described for the preparation of **3a** and **3b**.

The second goal of this work was the generation of pro-ligands suitable for the formation of mesoionic or ‘abnormal’ N-heterocyclic carbenes in combination with ‘normal’ NHCs. To this end, compounds **3a**, **3b**, **4a** and **4b** were alkylated at the N3 position of the 1,2,3-triazole ring to generate the triazolium containing pro-ligands **5a**, **5b**, **6a** and **6b** respectively (Scheme 2).⁶² Initial attempts to alkylate the N3 position of the 1,2,3-triazole unit by refluxing a mixture of the chosen 1,2,3-triazole and an excess of iodomethane in acetonitrile were unsuccessful with ¹H NMR analysis showing only unreacted starting material. After several additional attempts, it was found that the reactions could be successfully carried out at elevated temperature in a sealed flask. Using this approach, a mixture of the chosen 1,2,3-triazoles (either **3a**, **3b**, **4a**, and **4b**) and an excess of iodomethane (acting as both a reactant and solvent) in a sealed reaction flask was heated to 80 °C (Scheme 2). In the case of pro-ligands **3b** and **4b**, a small amount of acetonitrile was also added to ensure the starting materials were fully dissolved. A similar method for the alkylation of the N3 position of 1,2,3-triazoles with iodomethane has been reported previously by Poulain⁶³ and 1,2,3-triazoles have also been alkylated at the N3 position using the methylating agent trimethylxonium tetrafluoroborate.⁶⁴



Scheme 2: Alkylation at the N3 position of the triazole unit for class **I** ligands (**3a** and **3b**) (Upper panel) and class **II** ligands (**4a** and **4b**) (Lower panel).

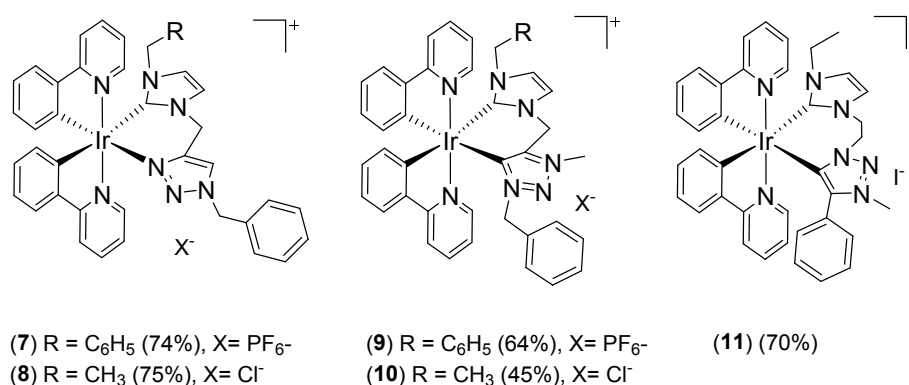
The ¹H NMR spectra of the imidazolium salt pro-ligands were relatively simple with a characteristic imidazolium pro-carbenic proton signal which resonated as a downfield shifted peak at 9.16, 9.08, 9.35, 9.20, 9.19, 9.37 and 9.30 ppm for pro-ligands **3a**, **3b**, **4a**, **5a**, **5b**, **6a** and **6b** respectively. For pro-ligands **3a**, **3b** and **4a** the C-H proton signals of the triazole group were in all cases the second most downfield shifted signals, resonating at 8.54, 8.54 and 8.28 for these molecules respectively. For pro-ligand **4b** the carbenic proton signal was observed at 7.42 ppm. Formation of the 1,2,3-triazolium unit resulted in a significant downfield shift of the triazolium C-H proton, with this proton resonating at 9.08, 9.13, 9.03 and 9.06 ppm for pro-ligands **5a**, **5b**, **6a**, and **6b** respectively. In each case, the base peak observed in the high-resolution mass spectra for the pro-ligands **3a-4b** corresponded to the mono-cationic imidazolium salt i.e. *m/z* 330.1713 [C₂₀H₂₀N₅]⁺ for **3a**. While for the imidazolium / 1,2,3-triazolium pro-ligands **5b-6b**, the base peak corresponded to a mono-cation consisting of the di-cationic pro-ligand in combination with one counter anion e.g. *m/z* 490.1589 [C₂₁H₂₃N₅]⁺PF₆⁻ for **5a** and *m/z* 410.0837 [C₁₆H₂₁N₅]⁺I⁻ for **5b**. The structures of pro-ligands **4a** and **5b** were confirmed by X-ray crystallography (see Structural Studies section).

Iridium complex synthesis

The Ir(III) N-heterocyclic carbene complexes were prepared utilizing a silver trans-metalation protocol. First developed by Lin and co-workers in 1998, the silver trans-metalation process involves *in situ* deprotonation of the imidazolium / triazolium unit and formation of an intermediate Ag(I) complex using Ag₂O.^{65, 66} The Ir(III) complexes were synthesized by introduction of the Ir(III) precursor [Ir(ppy)₂Cl]₂ (where ppy is 2-phenylpyridine). Based on the ligand structures it is expected

upon binding to the metal centre that pro-ligands **3a** and **3b** would produce seven-membered chelate rings, with coordination via the N2 position of the 1,2,3-triazole group. While for pro-ligands **4a** and **4b**, a six-membered chelate ring would be formed with coordination at the N3 position of the 1,2,3-triazole group.⁶⁷ Synthetic studies showed that Ir(III) complexes could only be prepared for pro-ligands **4a** and **4b** (Scheme 3). It is likely that complexes could not be prepared for pro-ligands **3a** and **3b** because of the larger chelate ring size and the known lower electron density at the N2 position of the 1,2,3-triazole resulting in this position binding less strongly to the metal centre.⁶⁸⁻⁷⁰

In contrast to the 1,2,3-triazole containing ligands, the alkylated triazolium pro-ligands (**5a**, **5b**, **6a**, and **6b**) were efficiently metallated regardless of the chelate ring size (Scheme 3). This is consistent with previously reported results, where 1,2,3-triazolylienes have been shown to be generally more efficient donors than imidazolidines.⁷¹ In the case of complex **5a**, analysis of the crude reaction mixture by ¹H NMR showed evidence for the formation of the complex, however, despite several attempts, the complex could not be satisfactorily purified. The structures of the successfully prepared Ir(III) complexes are shown in Scheme 3.



Scheme 3. Structures of Ir(III) complexes **7-11** synthesized in this work.

The expected number of signals were observed in the ¹H and ¹³C NMR spectra for the Ir(III) complexes **7-11** consistent with the low-symmetry structures. As expected, ¹H NMR analysis revealed the absence of the azolium pro-carbenic protons indicating deprotonation and coordination of the NHC groups to the Ir(III) metal centres. All complexes prepared were mono-cationic and analysis by high-resolution mass spectrometry showed a base peak in each case which corresponded to the complex ion e.g. *m/z* 830.2579 [C₄₂H₃₅IrN₇]⁺ in the case for **7**.

Structural Studies

View Article Online
DOI: 10.1039/C9DT01362H

The X-ray crystal structures of the pro-ligands **4a** and **5b** and the Ir(III) complex **11** are illustrated in Figures 2 and 3 respectively and the crystallographic data for these compounds are tabulated in Table S1 (Electronic Supplementary Information). Compound **4a** displays a short hydrogen-bonding interaction of 2.397(3) Å between the imidazolium proton (H1) and a fluorine atom of the hexafluorophosphate counterion (F10). The structure of **5b** confirms that this molecule is dicationic, with the imidazolium unit being linked to the triazolium group via an ethyl group. Both cationic azolium rings display hydrogen bonding interactions with the iodide counterions, with distances of 2.8979(3) Å for H18 (imidazolium) - I1 and 2.7773(3) Å for H24 (triazolium) - I4. The molecular structure of complex **11** shows a distorted octahedral coordination geometry about the Ir atom, with the coordination sphere composed of two cyclometalated 2-phenylpyridine (ppy) ligands in combination with the bidentate imidazolylidene / 1,2,3-triazolylidene ligand. In each case, the pyridine groups of the cyclometalated ppy ligands are trans with respect to one another. The Ir-C_{NHC} bond distances for the imidazolylidene and 1,2,3-triazolylidene donors are similar with these being 2.11555(5) Å (Ir1-C1) and 2.13457(4) Å (Ir1-C6) for these groups respectively. The ethyl linker group of the bidentate NHC ligand adopts a staggered conformation and there is a short interaction between one of the methylene hydrogen atoms (H4b) and the pyridine nitrogen atom (N7) of one of the ppy ligands of 2.37300(7) Å.

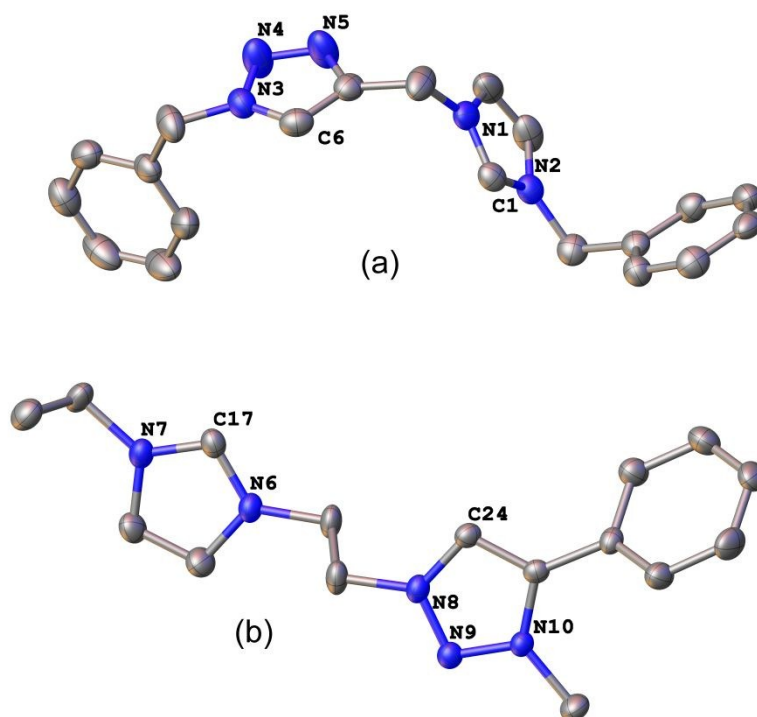


Figure 2. Representations of the cations found in the X-ray crystal structures of (a) **4a** and (b) **5b**. The hydrogen atoms, anions and solvent of crystallization have been omitted for clarity. Thermal ellipsoids are shown at 40% probability. Selected bond lengths for **4a**: N3-C6 = 1.326(7) Å, N3-N4 = 1.338(6) Å, N4-N5 = 1.305(6) Å, N1-C1 = 1.320(6) Å, N2-C1 = 1.329(6) Å. Selected bond lengths for **5b**: N7-C17 = 1.323(3) Å, N6-C17 = 1.311(4) Å, N8-C24 = 1.354(3) Å, N8-N9 = 1.307(3) Å, N9-N10 = 1.314(3) Å.

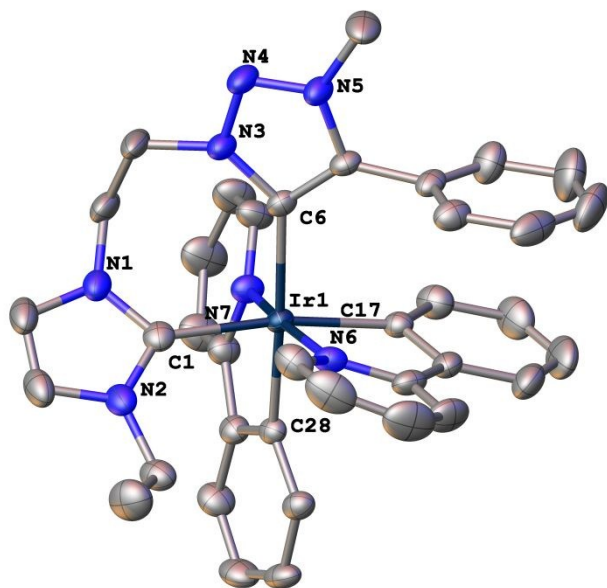


Figure 3. X-ray crystal structure of the Ir(III) complex **11**. The hydrogen atoms the anion and solvent of crystallization have been omitted for clarity. Thermal ellipsoids are shown at 40% probability. Selected bond lengths: Ir1-C17 = 2.053(4)Å, Ir1-C1 2.116(5)Å, Ir1-C6 = 2.134(4) Å, Ir1-C28 = 2.054(4) Å, Ir1-N6 = 2.041(4) Å, Ir1-N7 2.056(4) Å.

Photophysical and electrochemical studies

The electronic absorption and emissive properties of the Ir(III) complexes (**7-11**) were examined and the results are summarised in Table 1. The five complexes **7-11** displayed similar absorption spectra (Figure S1, Electronic Supplementary Information) with intense absorption bands below 300 nm resulting from spin-allowed $^1(\pi \rightarrow \pi^*)$ ligand-centred (LC) transitions originating on the NHC and 2-phenylpyridine ligands. Lower-intensity bands were observed between 300 nm and 500 nm which can be assigned to metal-to-ligand charge transfer (MLCT) transitions. As has been previously reported, strong spin-orbit coupling from the Ir(III) centre promotes mixing of these charge-transfer transitions with the higher energy spin-allowed LC transitions.^{54, 72}

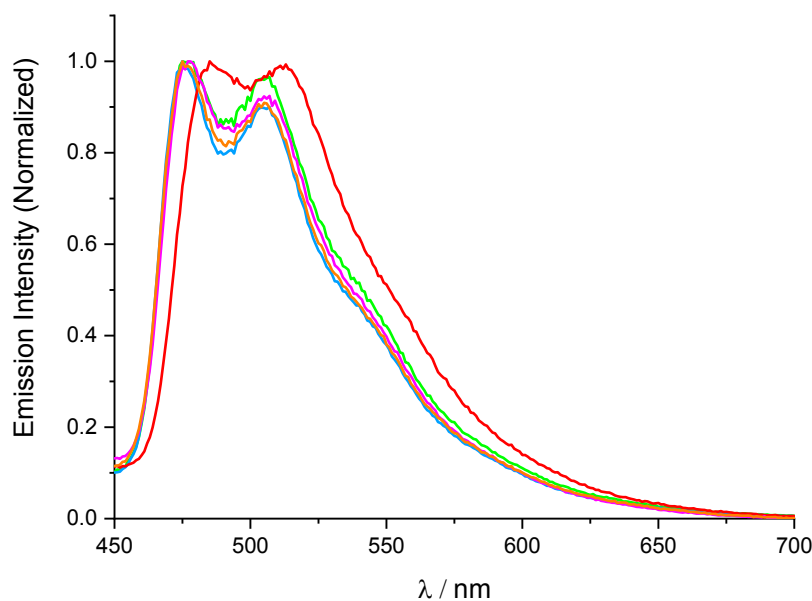


Figure 4. Normalised emission spectra for complexes **7-11** in (1×10^{-5} M in acetonitrile); **7** (green); **8** (pink); **9** (blue); **10** (orange) and **11** (red) ($\lambda_{\text{ex}} = 385$ nm for **7** and $\lambda_{\text{ex}} = 380$ nm for **8-11**).

The emission spectra for complexes **7-11** are shown in Figure 4. Strong spin-orbit coupling from the Ir metal centre facilitates intersystem crossing to triplet states with similar energy and enables the formation of an emissive mixed triplet excited state.⁷³ The spectra are similar for all complexes, exhibiting structured emission bands centred at ~ 490 nm in acetonitrile at room temperature. It is noteworthy that the nature of the substituent on either the triazole or imidazole rings had little effect on the emission properties of the complexes, with the exception of complex **11** for which the emission is bathochromically shifted by ~ 8 nm and shows a slight diminution of the higher order vibronic bands. These observations tell us that the ancillary ligands play a minor role in the transitions leading to the excited state, which are mainly associated to the phenylpyridine ligands

The photoluminescence quantum yields for the complexes were recorded from deoxygenated acetonitrile solutions (Table 1) and compounds **9** and **10** (57.4% and 50.0% respectively) showed the highest values. The brightness of complexes **9** and **10** compared to **7** and **8** can be credited to the presence of a methyl group in the N3 position of the 1,2,3-triazoles, which influences their abilities to destabilise thermally accessible metal centred non-emissive states. The lower quantum yield value obtained for compound **11** (8.8%) can be attributed to the iodide counter ion, which is well known for its propensity to efficiently quench luminescent emission.⁷⁴ The excited state lifetimes (Table 1) tend to support this trend showing a general enhancement when passing from aerated to deaerated

indicating an extreme sensitivity to the presence of oxygen, as has been observed previously for Ir(III) complexes of this type.⁷⁵ Upon degassing, compound **10** displays the longest lifetime of 1.43 μ s.

View Article Online
DOI: 10.1039/C9DT01362H

Table 1. Spectroscopic and electrochemical properties of Ir(III) complexes **7-11**

	λ_{\max}/nm ($\epsilon/\text{M}^{-1} \text{cm}^{-1}$) ^b		Photoluminescence λ_{\max}/nm ^c	Quantum yield $\phi_p/\%$ ^d	Lifetime (aerated) τ_p/ns ^e	Lifetime (deaerated) $\tau_p/\mu\text{s}$ ^f	E_{ox}/V^g	$E_{\text{red}}/\text{V}^g$
7	258 (39,000), (13, 100), (4,300)	310 380	475	5.9	34.66	0.37	0.78	(-2.48)
8	255 (42,500), (14,600), 390	310 (4,400)	485	4.1	31.80	0.88	0.76	-2.55
9	260 (40,300), (15,400), 380	310 (5,100)	475	57.4	46.81	0.69	(0.77)	-2.54
10^h	258 (30,100), (11,800), 380	310 (4,600)	475	50.0	43.12	1.43		
11	265 (43,700), (15,800), 390	320 (4.900)	485	8.8	32.44	0.85	0.78	(-2.44)

^aAll complexes 10^{-5} M in acetonitrile. ^b λ_{\max} is the position of the peak or shoulder in the absorbance profile, and ϵ is the molar absorptivity. ^cEmission corrected for variation in detector sensitivity with wavelength. ^dAbsolute quantum yields in deaerated solution. ^elifetimes in aerated solution and ^f in deaerated solution. ^g E_{ox} and E_{red} refer to $E_{1/2}$ values, peak potentials for irreversible processes are in parenthesis. ^hThe solubility of compound **10** in acetonitrile was insufficient to allow measurement of the cyclic voltammogram for this compound.

The electrochemical properties of complexes **7-9** and **11** were studied using cyclic voltammetry in degassed acetonitrile and the CVs for these complexes compared with that of $[\text{Ru}(\text{bpy})_3]^{2+}$ are shown in Figure 5 and the results are summarized in Table 1. The complexes each displayed an irreversible oxidation process related to $\text{Ir}^{3+}/\text{Ir}^{4+}$, with the forward peaks being much greater in magnitude than the reverse peaks at 0.1 V/s (i.e. $i_{p,\text{ox}} > i_{p,\text{red}}$). The oxidation processes (E_{ox}) all occurred at similar potentials within a short range ($\sim 40\text{mV}$) suggesting that the HOMO for each complex is mainly

delocalized over the metal and the phenyl group (of the ppy ligands) in each case. In the cathodic region each compound shows three one-electron ligand reductions at potentials more negative than the bipyridine reductions of $[\text{Ru}(\text{bpy})_3]^{2+}$. Only the second reduction (most likely associated with the 2-phenylpyridine ligands), shows a degree of reversibility, in agreement with results previously reported results for similar complexes.⁵⁵ The electrochemiluminescence (ECL) properties of each complex (**7-9** and **11**) were also tested by pulsing the applied potential between the oxidation and reduction potentials of the complexes (annihilation ECL). In each case, an ECL emission profile closely matching the photoluminescence spectrum obtained, however weak ECL was observed in most cases. Interestingly, the strongest ECL emitter was complex **8**, which gave an ECL efficiency of 39% relative to $[\text{Ru}(\text{bpy})_3]^{2+}$, despite having the lowest photoluminescence quantum yield. The co-reactant ECL abilities of the complexes was also tested by scanning past the oxidation potential in the presence of 10 mM tripropylamine (Figure S2, Electronic Supplementary Information). Similarly, the co-reactant ECL efficiency of each complex was negligible with the exception of **8**, for which the efficiency was 84% relative to the ruthenium standard. These results highlight the fact that the stability of the oxidised / reduced forms is often a more important factor than photophysical or thermodynamic considerations, for ECL efficiency. This is manifested in the voltammetric responses in Figure 5(a), where the oxidation process of **8** is significantly more chemically reversible compared to the other complexes, (notwithstanding that the response is somewhat convoluted with an irreversible peak for the oxidation of the chloride counterion).

View Article Online
DOI: 10.1039/C9DT01624H

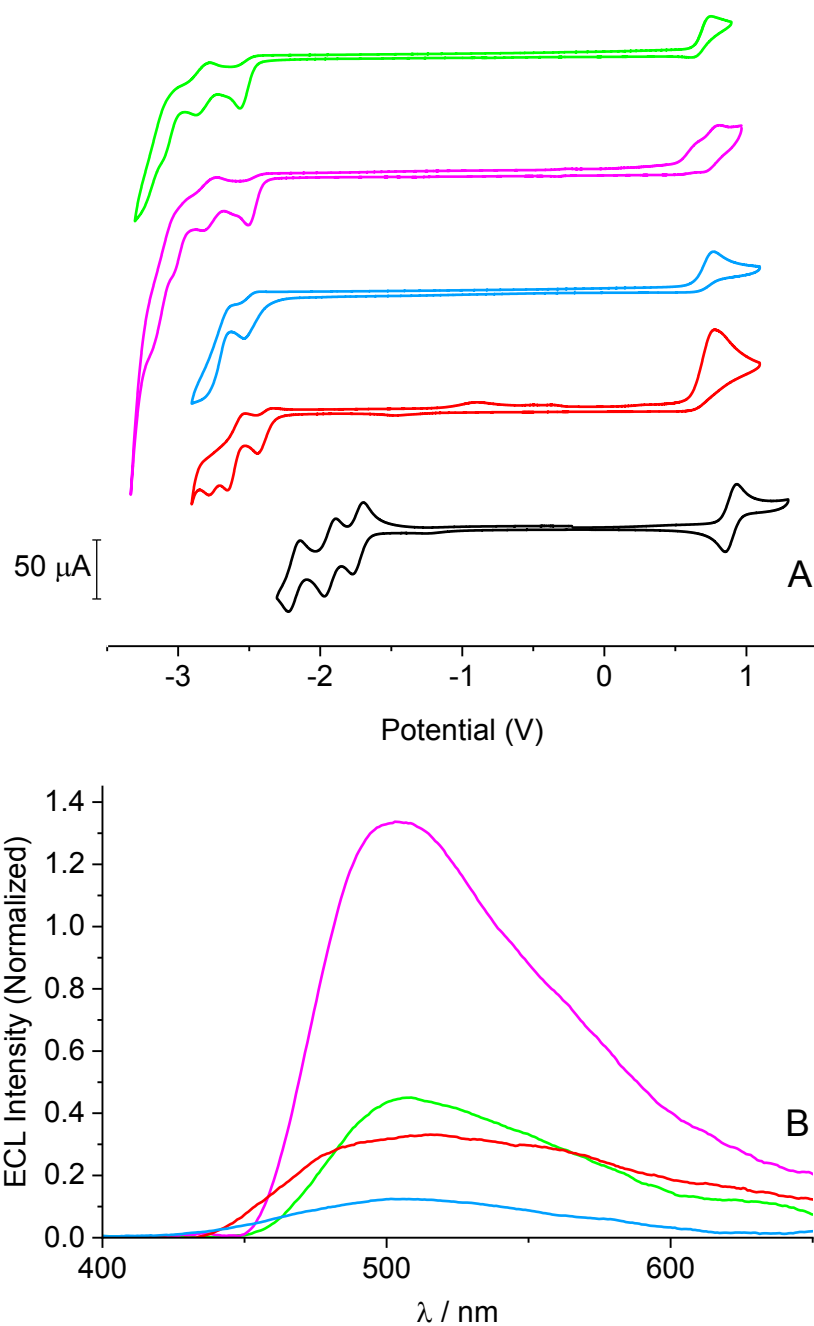


Figure 5. (A) Cyclic voltammetric responses for complexes **7-9**, **11** and [Ru(bpy)₃]²⁺; **7** (green); **8** (pink); **9** (blue); **11** (red) and [Ru(bpy)₃]²⁺ (black) using a glassy carbon working electrode at a scan rate of 0.1 V s⁻¹. Complex concentrations were 1 mM in acetonitrile containing 0.1 M [Bu₄N][PF₆] as supporting electrolyte. (B) ECL spectra produced via annihilation between the oxidized and reduced forms of the complexes. All iridium complexes are 10⁻⁴ M solution in acetonitrile containing 0.1 M [Bu₄N][PF₆]. Intensities have been normalized to [Ru(bpy)₃]²⁺ to reflect ECL quantum efficiencies; (green) **7**; (pink) **8**; (blue) **9**; (red) **11**.

Cell Imaging Studies

View Article Online
DOI: 10.1039/C9DT01362H

We are interested in the potential application of these Ir(III) complexes as luminescent probes for cell imaging studies and complexes **8** and **11** were selected for these preliminary imaging studies due to their good solubility in aqueous media. The uptake and distribution of these compounds were evaluated in A549 human lung adenocarcinoma basal epithelial cells. The cells were treated with either complexes **8** (100 μM) or **11** (50 μM) and the imaging experiments were begun immediately after complex addition. To avoid prolonged exposure to the laser a new section of cells was imaged at each time interval (5 min after complex addition and then at 15-minute intervals for 1 hour). Differential image contrast (DIC) and luminescent images of the epithelial cells 15 minutes after treatment are shown in Figure 6. The luminescence images show good uptake of the complexes into the cells and intracellular distribution consistent with specific organellar staining. As these compounds carry a cationic charge it was anticipated that they would display selective uptake into mitochondria. To test this hypothesis, co-localisation studies were performed with the commercial mitochondrial dye Mitotracker CMXRos. The merged images for the luminescence complex and Mitotracker (Figure 6) are consistent with co-localisation, suggesting mitochondrial uptake for these Ir(III) compounds.

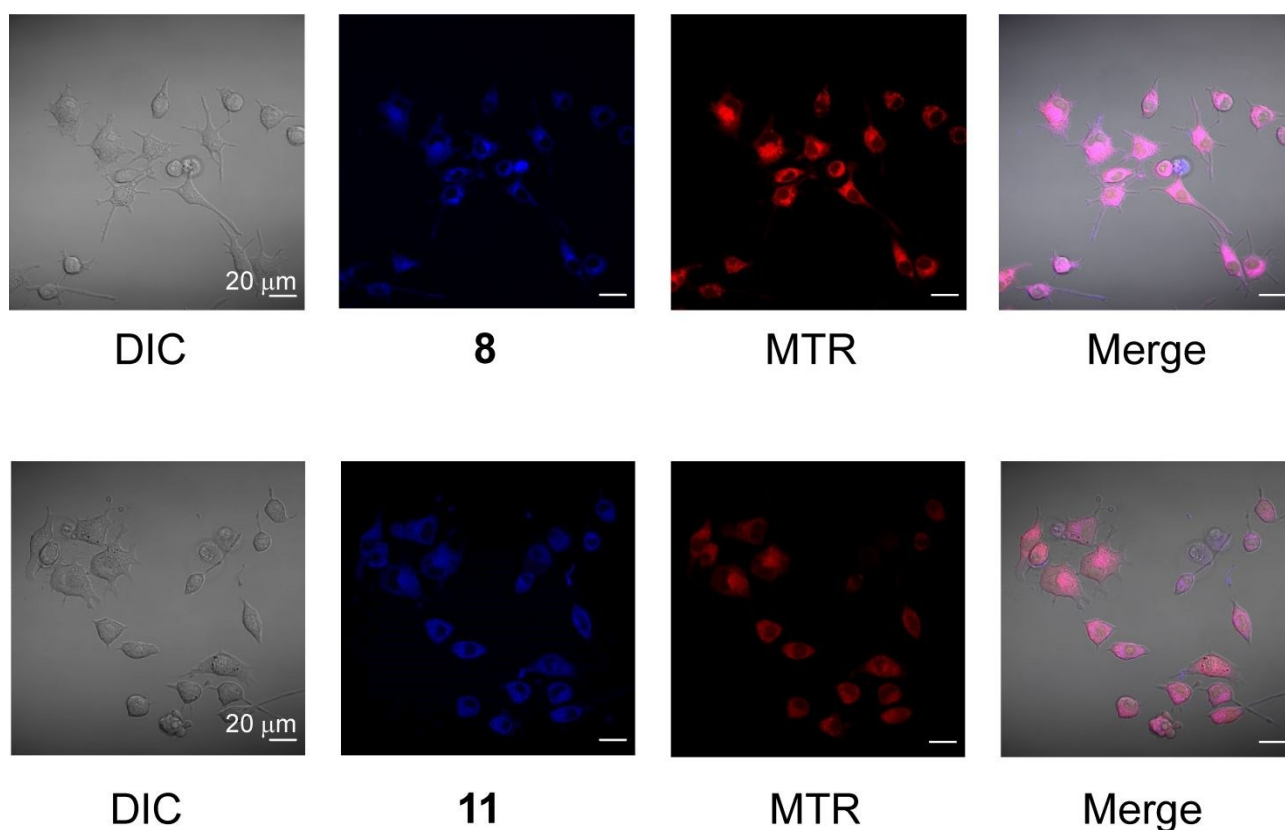


Figure 6. Live cell microscopy images of A549 human lung adenocarcinoma basal epithelial cells treated with complexes **8** (100 μM) (upper panel) and **11** (50 μM) (lower panel) and Mitotracker

CMXRos. From left to right: DIC, complex luminescence ($\lambda_{\text{ex}} = 405 \text{ nm}$), Mitotracker CMXRos luminescence ($\lambda_{\text{ex}} = 561 \text{ nm}$) and merged images.

View Article Online
DOI: 10.1039/C9DT01362H

Although these complexes demonstrated high levels of cell permeability and mitochondrial localization, they unfortunately also showed moderate cytotoxicity at the concentrations studied. Complex **8** was evaluated at 100 μM with cell viability decreasing from 89% at 15 min to 0% by 75 min. Similarly, viability of cells treated with complex **11** at 50 μM decreased from 80% at 15 min to 0% by 60 min. However, based on the results obtained in these studies, it is expected that lower concentrations the Ir(III) complexes that do not compromise cell viability, will still offer suitable luminescence intensity for cell imaging.

Conclusion

A series of bidentate imidazolium salt/1,2,3-triazole pro-ligands were prepared using the Cu(I) catalyzed azide-alkyne cycloaddition or 'click' reaction. For safety reasons, the required azide functionalized imidazolium salt precursors were formed *in situ* from the corresponding alkyl halides and in the same reaction pot, the 'click' reaction was carried out to introduce the triazole unit. In the case of the imidazolium salts functionalized with terminal alkyne groups, the cycloaddition reaction was carried out using benzylazide to form the 1,2,3-triazole unit. The 1,2,3-triazole group of these substituted imidazolium salts was then methylated using iodomethane to give a series of imidazolium/1,2,3-triazolium pro-ligands. Both classes of pro-ligands were then used to prepare five heteroleptic luminescent Ir(III) complexes. The photophysical properties of the complexes were evaluated and the quantum yields ranged from 4.1% to 57.4%. Electrochemical investigations revealed one formally Ir(III/IV) oxidation process and several ligand based reductions in each case. Some of the complexes displayed moderate annihilation or co-reactant ECL, depending on the reversibility of the electrochemical processes involved. Finally, due to the very well-known synthetic versatility of the 'click' reaction for conjugation processes including the linkage of molecular probes to biomolecules, it is our intention to utilize the 'click reactions' to prepare pro-ligands and to couple these molecules to biologically active molecules thereby yielding targeted luminescent molecular probes. With this in mind, a preliminary evaluation of two Ir(III) complexes as luminescent probes for live cell imaging studies was undertaken. The complexes are cationic and showed high levels of cell permeability in A549 human lung adenocarcinoma basal epithelial cells and co-localisation studies using Mitotracker CMXRos showed probable mitochondrial localisation. These studies show the significant potential for utilizing the click reaction for the synthesis of luminescent Ir(III) complexes for bioanalytical applications.

Experimental section

General Procedures. All reagents were purchased from Sigma-Aldrich or Alfa Aesar and were of analytical grade or higher and were used without further purification unless otherwise stated. All manipulations were performed under nitrogen unless otherwise stated. NMR spectra were recorded on either a Bruker Avance ARX-300 (300.14 MHz for ^1H , 75.48 MHz for ^{13}C) or a Bruker Avance ARX-400 (400.13 MHz for ^1H , 100.61 MHz for ^{13}C) or a Bruker Avance ARX-500 (500.13 MHz for ^1H , 125.77 MHz for ^{13}C) spectrometer and were internally referenced to solvent resonances. Mass spectra were obtained using a Bruker Esquire6000 mass spectrometer fitted with an Agilent electrospray (ESI) ion source. UV-visible spectra were recorded using an Agilent Technologies Cary 300 UV-visible spectrophotometer using quartz cuvettes (1 cm). Fluorescence spectra were recorded on a Varian Cary Eclipse spectrofluorimeter (5 nm band pass, 1 nm data interval, PMT voltage: 600 V) using quartz cuvettes (1 cm). All compounds were prepared in air unless otherwise specified.

X-ray Crystallography. Single crystals of the pro-ligands **4a** and **5b** and Ir(III) complex **11** suitable for X-ray diffraction studies were grown by slow diffusion of ether into DCM solutions (**4a** and **11**) and slow diffusion of ether into acetonitrile solution (**5b**). Crystallographic data for all structures determined are given in Table S1. For all samples, crystals were removed from the crystallization vial and immediately coated with paratone oil on a glass slide. A suitable crystal was mounted in Paratone oil on a glass fiber and cooled rapidly to 173 K in a stream of cold N_2 using an Oxford low-temperature device. Diffraction data were measured using an Oxford Gemini diffractometer mounted with $\text{Mo-K}\alpha$ $\lambda = 0.71073 \text{ \AA}$ and $\text{Cu-K}\alpha$ $\lambda = 1.54184 \text{ \AA}$. Data were reduced and corrected for absorption using the CrysAlis Pro program.⁷⁶ The SHELXL2013-2⁷⁷ program was used to solve the structures with Direct Methods, with refinement by the Full-Matrix Least-Squares refinement techniques on F^2 . The non-hydrogen atoms were refined anisotropically and hydrogen atoms were placed geometrically and refined using the riding model. Coordinates and anisotropic thermal parameters of all non-hydrogen atoms were refined. All calculations were carried out using the program Olex².⁷⁸ Further XRD details are provided in the Electronic Supplementary Information. CCDC 1905286-1905288 contains the supplementary crystallographic data for this paper. These data can be obtained free of charge from The Cambridge Crystallographic Data Centre via <https://www.ccdc.cam.ac.uk/structures/>

Photophysical measurements. UV-visible spectra were collected using a Cary Series UV-visible spectrophotometer (Agilent) with a 1 cm path length quartz cuvette, a spectral bandwidth of 1 nm, signal averaging time of 0.1 sec, data interval of 0.25 nm, scan rate of 150 nm/min and baseline/zero corrected. Steady-state emission spectra were collected on a Nanolog (HORIBA Jobin Yvon IBH) spectrometer using a 1 cm quartz cuvette, a band pass of 2 nm, an increment of 1 nm and integration time of 0.04 second. A 450 W Xenon-arc lamp was used to excite the complexes using a 1200 groves/mm grating blazed at 330 nm double excitation monochromator, a 1200 groves/mm grating

blazed at 500 nm emission monochromator and a thermoelectrically cooled TBX picosecond single-photon detector. A long pass filter KV399 was used on the emission side to block the excitation scatter peaks and the spectra were corrected for source intensity, gratings, detector response and sample optical density. 10 μM (Abs ~ 0.05 at 350 nm) solutions in an air-tight four-sided quartz cuvette were prepared in an N_2 glove box using acetonitrile free of any oxygen previously prepared via the freeze-pump-thaw (three times) method. Lifetimes (10 μM solutions) were measured using the time-correlated single photon counting (TCSPC) option on the spectrometer and correlated by a time-to-amplitude converter (TAC) in forward TAC mode. Nanoled 340 (344 nm) and Nanoled 460 (451 nm) lasers were pulsed at 100 kHz repetition rate with the emission band width set to 5 nm. Signals were collected using a FluoroHub counter and the data analyzed using DAS6 software (HORIBA Jobin Yvon IBH). Fitting of the curves was assessed by minimizing χ^2 (0.95-1.2) and visual inspection of the weighted residuals. For long lifetimes this involved fitting to the tail region by omitting the delta prompt. Spectra for absolute quantum yields were measured at room temperature ($22 \pm 2^\circ\text{C}$) with a Quanta-phi HORIBA Scientific 6 inch diameter integrating sphere connected to the Nanolog via optical fibres. The complexes were excited using a 450 W Xenon lamp and detected with a liquid nitrogen cooled Symphony II (model SII-1LS-256-06) CCD. Absolute quantum yields were calculated by the 4-plot method using Fluorescence v3.5 software following the equation;

$$\phi_p = \frac{\text{Photons Out}}{\text{Photons In}} = \frac{(E_c - E_a)/A}{L_a - L_c} \quad (1)$$

where E_c is the integrated luminescence of the sample, E_a is the integrated luminescence of the blank, A is the area balance factor due to CCD integration time, L_a is the integrated excitation from the blank and L_c is the integrated excitation from the sample.

Electrochemistry. Electrochemical experiments were performed using a PGSTAT12 AUTOLAB electrochemical potentiostat (MEP Instruments, North Ryde, NSW, Australia) with Nova 1.8 software. A conventional three-electrode cell configuration housed in an N_2 atmosphere glovebox was used, consisting of a silver wire quasi-reference electrode, a platinum wire auxiliary electrode and a 3 mm diameter glassy carbon disc working electrode shrouded in Teflon (CH Instruments, Austin, TX, USA). The working electrode was polished with 0.3 μm then 0.05 μm alumina slurry on a felt pad, rinsed with Milli-Q water followed by acetone then sonicated in acetonitrile for 10 seconds followed by a final rinse in acetonitrile and dried with a stream of N_2 . Potentials were referenced to the ferrocene/ferrocenium couple measured in situ in each case. Stock solutions of the complexes were prepared at a concentration of 1.0 mM in freshly distilled oxygen-free acetonitrile and $[\text{Bu}_4\text{N}][\text{PF}_6]$ was added to give a concentration of 0.1 M of supporting electrolyte.

Electrochemiluminescence

Solutions were prepared with distilled acetonitrile, then deoxygenated by bubbling N₂ for 10 mins prior to and blanketed during measurements. Annihilation ECL was generated with a 3 mm diameter glassy carbon electrode submerged at a constant height (2 mm from the cell bottom) in a 0.5 mM solution of the complex containing 0.1 M [Bu₄N][PF₆] as supporting electrolyte. ECL was generated carrying out chronoamperometry experiments for 12 cycles with 0.25 s for each step potential at 0.1 V vs. the Ag wire past the oxidation peak potential and reduction potentials. An integration time of 6 s for the CCD detector was used for each ECL spectrum.

ECL signals were detected using the Nanolog CCD (detector used in spectroscopic measurements) coupled via the FL-3000 Fibre-Optic Adapter and fibre optic bundle to the underside of a custom-built light-tight Faraday cage. ECL efficiencies were evaluated by comparing the annihilation ECL of each complex with that of 1 mM [Ru(bpy)₃]²⁺ (set at 100 and corrected for charge passed) at the same concentration of supporting electrolyte and same pulsing.

Cell lines and Tissue Culture

A549 human lung adenocarcinoma basal epithelial cells were a kind gift from the Chen Laboratory, LIMS, Department of Biochemistry and Genetics, La Trobe University. Cells were cultured in RPMI-1640 supplemented with 10% fetal bovine serum (FBS) containing penicillin (50 U/ml and streptomycin (50 U/ml) (Life Technologies, Carlsbad, CA) and 0.2% (vol/vol) MycoZap (Lonza, Basel, Switzerland). Microscopy experiments were performed in FBS-free RPMI-1640 supplemented with 1% bovine serum albumin.

Confocal Laser Scanning Microscopy (CLSM)

On the day prior to imaging, A549 cells were seeded onto to 8-well live cell imaging Nunc™ Lab-Tek™ II chamber slides (Nunc, Rochester, NY) and allowed to adhere overnight. Prior to imaging, cells were stained with mitochondrial dye Mitotracker CMXRos (Invitrogen) as per the manufacturer's instructions. Cells were then imaged in the presence of complexes **8** (at 100 μM) and **11** (at 50 μM). Imaging took place at t = 0, 5 min and then at 15 min intervals for a total duration of 60 min for **8** and 75 min for **11**. A new area of cells was imaged at each interval on a Zeiss LSM 780 confocal microscope (Zeiss, Oberkochen, Germany) using a 63x oil immersion objective and 405 nm / 561 nm lasers. Microscope chamber was heated to 37°C with 5% CO₂. Images were then analyzed using Zen software (Zeiss).

Synthesis

3a A mixture of **1a** (1.00 g, 2.89 mmol) and NaN₃ (0.23 g, 13.47 mmol) were stirred in DMF/water (50 mL, 4:1 v/v) at 50 °C for 5 h under a N₂ atmosphere. To the reaction mixture phenyl acetylene

(0.26 mL, 2.41 mmol), CuI (0.11 g, 0.58 mmol) and anhydrous Na₂CO₃ (0.78 g, 7.34 mmol) were added and stirring was continued at RT overnight. The reaction mixture was filtered, and the solvent removed *in vacuo*. Acetone was added to the residue and the resulting crude product was collected. Recrystallization of the solid in acetonitrile gave the product as a pale yellow crystalline solid (0.60 g, 60%). ¹H NMR (400 Hz, *d*₆-DMSO): δ 4.78 (dd, 2H, *J* = 4.12, 6.12 Hz, CH₂), 4.95 (dd, 2H, *J* = 5.04, 7.08 Hz, CH₂), 5.39 (s, 2H, Bn-CH₂), 7.22-7.37 (m, 6H, H_{Ar}), 7.44-7.47 (m, 2H, H_{Ar}), 7.77-7.79 (d, 2H, *J* = 1.65 Hz, H_{imi}), 7.8-7.81 (m, 2H, H_{Ar}), 8.54 (s, 1H, H_{az}), 9.16 (s, 1H, H_{imi}). ¹³C NMR (100 Hz, *d*₆-DMSO): δ 49.20 (CH₂), 49.52 (CH₂), 52.34 (Bn-CH₂), 122.25 (C_{az}), 123.38 (C_{imi}), 123.53 (C_{imi}), 125.64 (C_{Ar}), 128.37 (C_{Ar}), 128.52 (C_{Ar}), 129.07 (C_q), 129.35 (C_{Ar}), 129.40 (C_{Ar}), 130.91 (C_{Ar}), 135.07 (C_q), 137.17 (C_{imi}), 146.99 (C_q). HRESI-MS⁺ (CH₃OH): *m/z* 330.1713 [C₂₀H₂₀N₅]⁺ calcd. 330.1713.

3b This compound was prepared using the same procedure as that described for **3a** from **1b** (1.12 g, 1.72 mmol), NaN₃ (0.385 g, 2.58 mmol), phenyl acetylene (0.35 mL, 1.38 mmol), CuI (0.15 g, 0.34 mmol) and anhydrous Na₂CO₃ (1.25 g, 5.17 mmol). The crude product was recrystallised from a mixture of acetonitrile and ether yielding the product as a pale yellow crystalline solid (0.58 g, 43%). ¹H NMR (400 Hz, *d*₆-DMSO): δ 1.33 (t, 3H, *J* = 8.0 Hz, CH₃), 4.16 (q, 2H, *J* = 8.0, 12.0 Hz, CH₂), 4.75 (t, 2H, *J* = 4.0 Hz, CH₂), 4.94 (t, 2H, *J* = 4.0 Hz, CH₂), 7.34 (t, 1H, *J* = 8.0 Hz, H_{Ar}), 7.45 (t, 2H, *J* = 8.0 Hz, H_{Ar}), 7.69 (s, 1H, H_{imi}), 7.78-7.79 (m, 2H, H_{Ar}), 7.81 (s, 1H, H_{imi}), 8.54 (s, 1H, H_{az}), 9.08 (s, 1H, H_{imi}). ¹³C NMR (100 Hz, *d*₆-DMSO): δ 15.1 (CH₃), 44.3 (CH₂), 48.6 (CH₂), 49.1 (CH₂), 121.8 (C_{Az}), 122.4 (C_{imi}), 122.6 (C_{imi}), 125.1 (C_{Ar}), 128.0 (C_{Ar}), 128.9 (C_{Ar}), 130.4 (C_q), 136.2 (C_{imi}), 146.5 (C_q). HRESI-MS⁺ (CH₃OH): *m/z* 268.1554 [C₁₅H₁₈N₅]⁺ calcd. 268.1557.

4a A solution of benzyl chloride (0.22 mL, 1.82 mmol) and NaN₃ (0.14 g, 2.18 mmol) in a mixture of DMF/water (50 mL, 4:1 v/v) were stirred at 50 °C for 5 h under a N₂ atmosphere. Compound **2a** (0.47 g, 1.38 mmol), CuI (0.058 g, 0.30 mmol) and anhydrous Na₂CO₃ (0.48 g, 4.54 mmol) were added and the resulting mixture was stirred at RT overnight. The reaction mixture was filtered, and the solvent removed *in vacuo*. Acetone was then added, and the solution was filtered, and the solvent removed from the filtrate *in vacuo*. The crude product was triturated with ether to give the title compound (0.48 g, 76%). ¹H NMR (400 Hz, *d*₆-DMSO): δ 5.42 (s, 2H, CH₂), 5.52 (s, 2H, CH₂), 5.62 (s, 2H, CH₂), 7.31-7.42 (m, 10H, H_{Ar}), 7.78 (dt, 2H, *J* = 1.88, 9.92 Hz, H_{imi}), 8.28 (s, 1H, H_{az}), 9.35 (s, 1H, H_{imi}). ¹³C NMR (100 Hz, *d*₆-DMSO): δ 43.8 (CH₂), 55.0 (CH₂), 53.0 (CH₂), 122.7 (C_{imi}), 123.0 (C_{imi}), 124.6 (C_{az}), 128.0 (C_{Ar}), 128.3 (C_{Ar}), 128.3 (C_{Ar}), 128.8 (C_{Ar}), 129.0 (C_q), 134.7 (C_q), 135.7 (C_q), 136.3 (C_{imi}), 140.6 (C_q). HRESI-MS⁺ (CH₃OH): *m/z* 330.1712 [C₂₀H₂₀N₅]⁺ calcd. 330.1713.

4b To a solution of **2b** (0.456 g, 2.67 mmol) in a mixture of DMF/water (20 mL, 4:1 v/v) was added benzyl azide (0.40 mL, 3.21 mmol), CuI (0.102 g, 0.53 mmol) and anhydrous Na₂CO₃ (0.850 g, 8.02 mmol). This mixture was stirred at RT under an N₂ atmosphere overnight. The reaction mixture was filtered, and the solvent removed *in vacuo*. Acetone was then added to the residue and the solution was filtered and the solvent removed from the filtrate *in vacuo*. The crude product was then dissolved in CH₂Cl₂ and this solution was extracted with water. The aqueous layers were collected and dried and the residue was recrystallised from a mixture of isopropanol and ether followed by acetonitrile. (0.372 g, 46%). ¹H NMR (500 Hz, *d*₆-DMSO): δ 0.67 (t, 3H, *J* = 7.22 Hz, CH₃), 3.41 (q, 2H, *J* = 7.42, 15.21 Hz, CH₂), 4.71 (s, 2H, Bn-CH₂), 4.80 (s, 1H, CH₂), 6.53-6.59 (m, 6H, H_{Ar}, H_{Az}), 6.69 (d, 1H, *J* = 1.94 Hz, H_{imi}), 6.74 (d, 1H, *J* = 1.94 Hz, H_{imi}), 7.42 (s, 1H, H_{imi}). ¹³C NMR (125 Hz, *d*₆-DMSO): δ 5.9 (CH₃), 35.1 (CH₂), 36.6 (CH₂), 45.6 (CH₂), 113.7 (C_{imi}), 114.0 (C_{imi}), 116.7 (C_{imi}), 119.5 (C_{Ar}), 119.7 (C_{Ar}), 120.4 (C_{Ar}), 120.5 (C_{Az}), 120.6 (C_{Ar}), 126.1 (C_q). HRESI-MS⁺ (CH₃OH): *m/z* 268.1556 [C₁₅H₁₈N₅]⁺ calcd. 268.1557.

5a A mixture of **3a** (0.19 g, 0.46 mmol) and iodomethane (3 mL, 47.8 mmol) were prepared in an Ace pressure tube and the reaction was stirred at 80 °C for a week (after one day a dark red oil had formed). The flask was cooled to RT and the remaining iodomethane was then removed *in vacuo*. The residue was dissolved in a mixture of methanol and water (4.0 mL, 1:1 v/v) and a saturated aqueous solution of KPF₆ (~1 mL) was added to form a white solid. This solid was collected and washed with water (0.26 g, 87%). ¹H NMR (400 Hz, *d*₆-DMSO): δ 4.20 (s, 3H, CH₃), 4.85 (t, 2H *J* = 5.48 Hz, CH₂), 5.19 (t, 2H, *J* = 5.14 Hz, CH₂), 5.43 (s, 2H, Bn-CH₂), 5.39-5.40 (m 5H, H_{Ar}), 7.69-7.70 (m, 5H, H_{Ar}), 7.82 (t, 1H, *J* = 1.71 Hz, H_{imi}), 7.87 (t, 1H, *J* = 1.71 Hz, H_{imi}), 9.08 (s, 1H, H_{Az}), 9.20 (s, 1H, H_{imi}). ¹³C NMR (100 Hz, *d*₆-DMSO): δ 47.71 (CH₂), 52.15 (Bn-CH₂), 52.57 (CH₂), 122.32 (C_q), 123.07 (C_{imi}), 123.16 (C_{imi}), 128.23 (C_{Ar}), 128.84 (C_{Ar}), 129.03 (C_{Ar}), 129.23 (C_{Ar}), 129.52 (C_{Ar}), 129.57 (C_{imi}), 131.72 (C_{Ar}), 134.56 (C_q), 137.06 (C_{imi}), 142.49 (C_q). HRESI-MS⁺ (CH₃OH): *m/z* 490.1589 [C₂₁H₂₃N₅]⁺PF₆⁻ calcd. 490.1590.

5b This compound was prepared using the same procedure as that described for **5a** from **3b** (0.15 g, 0.43 mmol) dissolved in acetonitrile (2 mL) and iodomethane (3 mL, 47.7 mmol). The crude product was recrystallized from a mixture of acetonitrile and ether to give the compound as a white crystalline solid (0.17 g, 74%). ¹H NMR (400 Hz, *d*₆-DMSO): δ 1.42 (t, 3H, *J* = 4.0 Hz, CH₃), 4.22 (q, 2H, *J* = 4.0, 12.0 Hz, CH₂), 4.27 (s, 3H, CH₃), 4.86 (t, 2H, *J* = 4.0 Hz, CH₂), 5.21 (t, 2H, *J* = 4.0 Hz, CH₂), 7.68-7.80 (m, 5H, H_{Ar}), 7.81 (d, 1H, *J* = 1.69 Hz, H_{imi}), 7.86 (t, 1H, *J* = 1.55 Hz, H_{imi}), 9.13 (s, 1H, H_{Az}), 9.19 (s, 1H, H_{imi}). ¹³C NMR (100 Hz, *d*₆-DMSO): δ 15.0 (CH₃), 44.4 (CH₂), 47.5 (CH₂), 52.6 (CH₂), 122.4 (C_q), 122.6 (C_{imi}), 122.7 (C_{imi}), 129.3 (C_{Ar}), 129.4 (C_{Ar}), 129.6 (C_{Az}), 131.6 (C_{Ar}), 136.6 (C_{imi}), 142.4 (C_q). HRESI-MS⁺ (CH₃OH): *m/z* 410.0837 [C₁₆H₂₁N₅]⁺I⁻ calcd. 410.0836.

6a This compound was prepared using the same procedure as that described for **5a** from **4a** (0.211 g, 0.46 mmol) and iodomethane (3 mL, 47.7 mmol). The resulting residue was re-dissolved in CH_2Cl_2 and water (4.0 mL, 1:1) and a saturated aqueous solution of KPF_6 (~1 mL) was added. The organic layer was collected and washed with water (3 x 15 mL), dried over MgSO_4 and the solvent removed *in vacuo* yielding a sticky red residue. The residue was triturated with ether to give the title compound (72 mg, 25%). ^1H NMR (400 Hz, d_6 -DMSO): δ 4.31 (s, 3H, CH_3), 5.44 (s, 2H, CH_2), 5.80 (s, 2H, CH_2), 5.91 (s, 2H, CH_2), 7.41-7.46 (m, 10H, H_{Ar}), 7.86 (d, 2H, J = 12.4 Hz, H_{imi}), 9.03 (s, 1H, H_{Az}), 9.37 (s, 1H, H_{imi}). ^{13}C NMR (100 Hz, d_6 -DMSO): δ 38.5 (CH_3), 40.5 (CH_2), 52.2 (CH_2), 56.3 (CH_2), 123.0 (C_{imi}), 123.2 (C_{imi}), 128.4 (C_{Ar}), 128.9 (C_{Ar}), 129.0 (C_{Ar}), 129.1 (C_{Ar}), 129.4 (C_{Ar}), 131.0 (C_{Az}), 132.7 (C_{q}), 134.4 (C_{q}), 137.3 (C_{imi}), 137.6 (C_{q}). HRESI-MS⁺ (CH_3OH): m/z 490.1585 [$\text{C}_{21}\text{H}_{23}\text{N}_5$] PF_6 ⁺ calcd. 490.1595.

6b This compound was prepared using the same procedure as that described for **5a** from **4b** (0.202 g, 0.66 mmol) dissolved in acetonitrile (2 mL) and iodomethane (3 mL, 47.7 mmol). Water was added to the dark red residue and the resulting dark red precipitate was removed by filtration. The filtrate was dried *in vacuo* and the residue was recrystallised from methanol (5 mL). (0.101g, 28%). ^1H NMR (500 Hz, d_6 -DMSO): δ 1.44 (t, 3H, J = 7.14 Hz, CH_3), 4.22 (q, 2H, J = 7.42, 16.47 Hz, CH_2), 4.32 (s, 3H, CH_3), 5.81 (s, 2H, CH_2), 5.91 (s, 2H, CH_2), 7.43-7.49 (m, 5H, H_{Ar}), 7.84 (s, 1H, H_{imi}), 7.89 (s, 1H, H_{imi}), 9.06 (s, 1H, H_{Az}), 9.30 (s, 1H, H_{imi}). ^{13}C NMR (125 Hz, d_6 -DMSO): δ 14.9 (CH_3), 38.6 (CH_3), 40.5 (CH_2), 44.6 (CH_2), 56.3 (CH_2), 122.7 (C_{imi}), 122.8 (C_{imi}), 129.0 (C_{Ar}), 129.2 (C_{Ar}), 129.4 (C_{Ar}), 131.0 (C_{Az}), 132.7 (C_{q}), 136.9 (C_{q}), 137.7 (C_{imi}). HRESI-MS⁺ (CH_3OH): m/z 410.0836 [$\text{C}_{16}\text{H}_{21}\text{N}_5$] I^+ calcd. 410.0836.

7 A mixture of **4a** (0.050 g, 0.11 mmol), Ag_2O (32 mg, 0.14 mmol) and $[\text{Ir}(\text{ppy})_2\text{Cl}]_2$ (59 mg, 0.06 mmol) in 1,2-dichloroethane (20 mL) was stirred at 80 °C in the dark overnight. The hot mixture was filtered through a plug of Celite and the solvent removed from the filtrate *in vacuo*. The product was purified by column chromatography (10% methanol/ CH_2Cl_2) on silica gel and the title compound was obtained as a yellow crystalline solid (68 mg, 74%). ^1H NMR (400 Hz, d_6 -DMSO): δ 4.49 (q, 2H, J = 15.88, 24.43 Hz), 5.22 (d, 1H, J = 16.25 Hz), 5.49 (q, 2H, J = 14.72, 18.50 Hz), 5.64 (d, 1H, J = 16.55 Hz), 5.96 (d, 1H, J = 7.51 Hz), 6.19 (dd, 3H, J = 1.53, 7.08 Hz), 6.64 (t, 1H, 6.90 Hz), 6.74-6.78 (m, 2H), 6.86 (t, 1H, J = 7.45 Hz), 6.96-7.07 (m, 6H), 7.11 (d, 1H, J = 1.98 Hz), 7.23-7.32 (m, 5H), 7.61-7.70 (m, 4H), 7.76 (d, 1H, J = 5.19 Hz), 7.84 (d, 1H, J = 8.31 Hz), 7.94 (t, 1H, J = 8.12 Hz), 8.10 (d, 1H, J = 7.82 Hz), 8.42 (s, 1H), 8.47 (d, 1H, J = 4.95 Hz). ^{13}C NMR (100 Hz, d_6 -DMSO): δ 44.23, 50.80, 53.94, 199.56, 120.02, 120.53, 121.72, 123.86, 124.32, 124.73, 124.87, 125.13, 126.63, 127.84, 127.88, 128.35, 128.69, 129.01, 129.05, 130.26, 131.08, 134.70, 137.02, 138.27, 141.10,

143.40, 144.39m 149.33, 150.68, 153.08, 161.46, 166.56, 167.23, 169.14. HRESI-MS⁺ (CH₃OH): *m/z* 830.2579 [C₄₂H₃₅IrN₇]⁺ calcd. 830.2578.

View Article Online
DOI: 10.1039/C9DT01362H

8 This compound was prepared using the same procedure as that described for **7** from **4b** (0.075 g, 0.25 mmol), Ag₂O (0.068 g, 0.30 mmol) and [Ir(ppy)₂Cl]₂ (0.106 g, 0.1 mmol). The crude product was triturated several times with acetone and then dried *in vacuo*. (87 mg, 55%). ¹H NMR (500 Hz, *d*₆-DMSO): δ 0.31 (t, 3H, *J* = 6.72 Hz), 3.45-3.49 (m, 1H), 5.27 (d, 1H, *J* = 16.42 Hz), 5.43-5.54 (m, 2H), 6.01 (d, 1H, *J* = 7.95 Hz), 6.27 (d, 1H, *J* = 7.51 Hz), 6.73 (t, 1H, *J* = 7.51 Hz), 6.78 (t, 1H, *J* = 7.07 Hz), 6.84-6.92 (m, 4H), 7.15-7.21 (m, 2H), 7.24-7.30 (m, 3H), 7.32 (s, 1H), 7.57 (s, 1H), 7.73 (d, 1H, *J* = 7.51 Hz), 7.82 (d, 1H, *J* = 7.95 Hz), 7.96 (t, 2H, *J* = 7.95 Hz), 8.07 (d, 1H, *J* = 5.74 Hz), 8.15 (d, 1H, *J* = 7.95 Hz), 8.21 (d, 1H, *J* = 5.74 Hz), 8.26 (d, 1H, *J* = 7.95 Hz), 8.45 (s, 1H). ¹³C NMR (125 Hz, *d*₆-DMSO): δ 15.6, 43.5, 44.0, 53.8, 119.8, 120.0, 120.6, 121.5, 121.7, 122.7, 123.7, 123.8, 123.9, 124.5, 125.0, 127.6, 128.3, 128.7, 129.1, 130.9, 134.7, 137.5, 138.2, 141.0, 143.5, 144.6, 150.1, 151.1, 152.6, 161.7, 165.6, 167.1, 169.2. HRESI-MS⁺ (CH₃OH): *m/z* 768.2420 [C₃₇H₃₃IrN₇]⁺ calcd. 768.2421.

9 This compound was prepared using the same procedure as that described for **7** from **6a** (0.072 g, 0.12 mmol), Ag₂O (0.068 g, 0.29 mmol), and [Ir(ppy)₂Cl]₂ (0.062 g, 0.058 mmol) in a mixture of CH₂Cl₂/methanol (20 mL, 1:1, v/v). The product was purified by column chromatography (CH₂Cl₂, then 1-5% methanol/CH₂Cl₂) on silica gel. The title compound was obtained as a yellow solid which was then recrystallized in CH₂Cl₂ (74 mg, 64%). ¹H NMR (500 Hz, *d*₆-DMSO): δ 4.21 (s, 3H), 4.61 (d, 1H, *J* = 15.42 Hz), 4.75 (d, 1H, *J* = 15.18 Hz), 4.85 (d, 1H, *J* = 15.42 Hz), 4.94 (d, 1H, *J* = 15.18 Hz), 5.57 (d, 1H, *J* = 16.89 Hz), 5.65 (d, 1H, *J* = 16.89 Hz), 6.09 (dd, 1H, *J* = 0.86, 7.59 Hz), 6.14 (dd, 1H, *J* = 0.86, 7.53 Hz), 6.26 (d, 2H, *J* = 7.28 Hz), 6.31 (d, 2H, *J* = 7.16), 6.55 (td, 1H, *J* = 1.19, 7.53 Hz), 6.63-6.65 (m, 2H), 6.74-6.76 (m, 1H), 6.00-7.12 (m, 9H), 7.61-7.63 (m, 2H), 7.63 (d, 1H, *J* = 8.02 Hz), 7.93-7.96 (m, 2H), 8.26 (dd, 1H, *J* = 0.75, 5.78 Hz), 8.43 (dd, 1H, *J* = 0.80, 5.85 Hz). ¹³C NMR (125 Hz, *d*₆-DMSO): δ 51.16, 54.03, 123.06, 123.19, 123.79, 123.86, 124.19, 124.26, 125.02, 125.16, 126.16, 126.74, 126.83, 127.42, 127.67, 127.95, 128.34, 128.64, 134.52, 136.17, 136.88, 137.33, 137.40, 137.94, 142.12, 148.98, 150.27, 152.32, 154.40, 155.75, 156.60, 156.72, 157.61, 181.51. HRESI-MS⁺ (CH₃OH): *m/z* 844.2734 [C₄₃H₃₇IrN₇]⁺ calcd. 844.2734.

10 This compound was prepared using the same procedure as that described for **7** from **6b** (0.094 g, 0.017 mmol), Ag₂O (0.049 g, 0.21 mmol) and Ir(ppy)₂Cl]₂ (0.075 g, 0.07 mmol). The product was collected by filtration and washed with acetone. (57 mg, 45%). ¹H NMR (500 Hz, *d*₆-DMSO): δ 0.21 (t, 3H, *J* = 6.83 Hz), 3.47-3.51 (m, 1H), 3.83-3.87 (m, 1H), 4.22 (s, 3H), 4.49 (d, 1H, *J* = 15.74 Hz), 4.85 (d, 1H, *J* = 15.12 Hz), 5.34 (d, 1H, *J* = 16.84 Hz), 5.68 (d, 1H, *J* = 16.84 Hz), 6.16 (q, 2H, *J* = 7.34, 14.25 Hz), 6.22 (d, 2H, *J* = 7.34 Hz), 6.66 (t, 1H, *J* = 7.34 Hz), 6.70 (t, 1H, *J* = 6.91 Hz), 6.77-6.83 (m,

2H), 6.98-7.04 (m, 3H), 7.07 (t, 1H, $J=7.34$ Hz), 7.13 (t, 1H, $J=7.34$ Hz), 7.33 (d, 1H, $J=1.41$ Hz), 7.52 (d, 1H, $J=1.51$ Hz), 7.64-7.70 (m, 2H), 7.73 (d, 1H, $J=7.63$ Hz), 7.87-7.90 (m, 2H), 8.00 (d, 1H, $J=5.62$ Hz), 8.11 (d, 1H, $J=8.03$ Hz), 8.57 (d, 1H, $J=5.62$ Hz). ^{13}C NMR (125 Hz, d_6 -DMSO): δ 15.1, 36.6, 44.0, 44.5, 53.7, 119.8, 119.9, 120.7, 120.9, 121.6, 122.7, 123.6, 123.8, 124.9, 125.7, 127.0, 127.9, 128.7, 129.0, 130.4, 131.4, 135.6, 136.7, 137.2, 140.7, 144.1, 144.2, 152.0, 152.3, 163.0, 163.2, 164.1, 168.0, 168.8. HRESI-MS⁺ (CH₃OH): m/z 782.2579 [C₃₈H₃₅IrN₇]⁺ calcd. 782.2578.

11 This compound was prepared using the same procedure as that described for **7** from **5b** (0.05 g, 0.093 mmol), Ag₂O (0.027 g, 0.11 mmol) and Ir(ppy)₂Cl₂ (0.05 g, 0.05 mmol). The product was recrystallized from acetone (59 mg, 70%). ^1H NMR (500 Hz, d_6 -DMSO): δ 0.31 (t, 3H, $J=7.16$ Hz), 3.40 (s, 3H), 3.48-3.54 (m, 1H), 3.64-3.71 (m, 1H), 4.35 (dd, 1H, $J=6.05, 15.95$ Hz), 4.65 (dd, 1H, $J=11.55, 15.95$ Hz), 4.75, (dd, 1H, $J=11.0, 14.85$ Hz), 5.28 (dd, 1H, $J=5.5, 15.4$ Hz), 5.69-5.74 (m, 2H), 6.18 (d, 1H, $J=8.25$ Hz), 6.31-6.40 (m, 3H), 6.58 (dd, 1H, $J=1.11, 8.10$ Hz), 6.62-6.67 (m, 2H), 6.77 (t, 1H, $J=7.39$ Hz), 7.01-7.20 (m, 3H), 7.21 (d, 1H, $J=2.02$ Hz), 7.27-7.30 (m, 1H), 7.34 (d, 1H, $J=1.92$ Hz), 7.49 (d, 1H, $J=7.49$ Hz), 7.70 (d, 1H, $J=8.30$ Hz), 7.82-7.85 (m, 1H), 7.88-7.92 (m, 1H), 7.97 (d, 1H, $J=8.30$ Hz), 8.24 (d, 1H, $J=5.87$ Hz), 9.02 (d, 1H, $J=5.77$ Hz). ^{13}C NMR (125 Hz, d_6 -DMSO): δ 15.66, 36.11, 44.54, 45.05, 55.72, 119.57, 119.69, 119.82, 120.23, 121.09, 121.33, 122.90, 123.27, 124.81, 127.23, 127.48, 127.70, 129.02, 131.91, 136.18, 136.99, 144.18, 145.42, 149.89, 154.45, 154.83, 160.68, 165.08, 165.49, 168.84, 168.91. HRESI-MS⁺ (CH₃OH): m/z 782.2579 [C₃₈H₃₅IrN₇]⁺ calcd. 782.2578.

Acknowledgments

The Australian Research Council is acknowledged for funding that supported part of this work (DP150102741) and the La Trobe University Bioimaging Platform for allowing us to conduct cell studies via Confocal Laser Scanning Microscopy (CLSM).

References

1. W. A. Herrmann and C. Köcher, *Angew. Chem. Int. Ed. in English*, 1997, **36**, 2162-2187.
2. M. G. Gardiner and C. C. Ho, *Coord. Chem. Rev.*, 2018, **375**, 373-388.
3. R. Zhong, A. C. Lindhorst, F. J. Groche and F. E. Kühn, *Chem. Rev.*, 2017, **117**, 1970-2058.
4. J.-Q. Liu, X.-X. Gou and Y.-F. Han, *Chem. Asian J.*, 2018, **13**, 2257-2276.
5. W. Wang, L. Cui, P. Sun, L. Shi, C. Yue and F. Li, *Chem. Rev.*, 2018, **118**, 9843-9929.
6. J. Yang, J. Liu, Y. Wang and J. Wang, *J. Incl. Phenom. Macrocycl. Chem.*, 2018, **90**, 15-37.
7. M. Elie, J. L. Renaud and S. Gaillard, *Polyhedron*, 2018, **140**, 158-168.
8. R. Visbal and M. C. Gimeno, *Chem. Soc. Rev.*, 2014, **43**, 3551-3574.
9. B. Dominelli, J. D. G. Correia and F. E. Kühn, *J. Organomet. Chem.*, 2018, **866**, 153-164.
10. S. A. Patil, S. A. Patil, R. Patil, R. S. Keri, S. Budagumpi, G. R. Balakrishna and M. Tacke, *Future Med. Chem.*, 2015, **7**, 1305-1333.

11. P.-H. Lanoë, J. Chan, G. Gontard, F. Monti, N. Armaroli, A. Barbieri and H. Amouri, *Eur. J. Inorg. Chem.*, 2016, **2016**.
View Article Online
DOI: 10.1039/C9DT01362H
12. P.-H. Lanoë, J. Chan, A. Groué, G. Gontard, A. Jutand, M.-N. Rager, N. Armaroli, F. Monti, A. Barbieri and H. Amouri, *Dalton Trans.*, 2018, **47**, 3440-3451.
13. A. J. Arduengo, R. L. Harlow and M. Kline, *J. Am. Chem. Soc.*, 1991, **113**, 361-363.
14. S. Gründemann, A. Kovacevic, M. Albrecht, J. W. Faller Robert and H. Crabtree, *Chem. Commun.*, 2001, **0**, 2274-2275.
15. G. Sini, O. Eisenstein and R. H. Crabtree, *Inorg. Chem.*, 2002, **41**, 602-604.
16. S. Gründemann, A. Kovacevic, M. Albrecht, J. W. Faller and R. H. Crabtree, *J. Am. Chem. Soc.*, 2002, **124**, 10473-10481.
17. E. Aldeco-Perez, A. J. Rosenthal, B. Donnadiou, P. Parameswaran, G. Frenking and G. Bertrand, *Science*, 2009, **326**, 556.
18. J. D. Crowley and P. H. Bandeen, *Dalton Trans.*, 2010, **39**, 612-623.
19. J. D. Crowley and D. A. McMorran, in *Click Triazoles*, ed. J. Košmrlj, Springer Berlin Heidelberg, Berlin, Heidelberg, 2012, **67**, pp. 31-83.
20. D. Huang, P. Zhao and D. Astruc, *Coord. Chem. Rev.*, 2014, **272**, 145-165.
21. H. Struthers, T. L. Mindt and R. Schibli, *Dalton Trans.*, 2010, **39**, 675-696.
22. C. M. Álvarez, L. A. García-Escudero, R. García-Rodríguez and D. Miguel, *Chem. Commun.*, 2012, **48**, 7209-7211.
23. M. Frutos, M. Gómez-Gallego, E. A. Giner, M. A. Sierra and C. Ramírez de Arellano, *Dalton Trans.*, 2018, **47**, 9975-9979.
24. G. Guisado-Barrios, J. Bouffard, B. Donnadiou and G. Bertrand, *Organometallics*, 2011, **30**, 6017-6021.
25. P. Mathew, A. Neels and M. Albrecht, *J. Am. Chem. Soc.*, 2008, **130**, 13534-13535.
26. L.-A. Schaper, X. Wei, S. J. Hock, A. Pöthig, K. Öfele, M. Cokoja, W. A. Herrmann and F. E. Kühn, *Organometallics*, 2013, **32**, 3376-3384.
27. H. C. Kolb, M. G. Finn and K. B. Sharpless, *Angew. Chem. Int. Ed.*, 2001, **40**, 2004-2021.
28. D. Astruc, L. Liang, A. Rapakousiou and J. Ruiz, *Acc. Chem. Res.*, 2012, **45**, 630-640.
29. P. A. Scattergood and P. I. P. Elliott, *Dalton Trans.*, 2017, **46**, 16343-16356.
30. D. Schweinfurth, L. Hettmanczyk, L. Suntrup and B. Sarkar, *Z. Anorg. Allg. Chem.*, 2017, **643**, 554-584.
31. Z.-J. Zheng, D. Wang, Z. Xu and L.-W. Xu, *Beilstein J. Org. Chem.*, 2015, **11**, 2557-2576.
32. A. Maisonial, P. Serafin, M. Traïkia, E. Debiton, V. Théry, D. J. Aitken, P. Lemoine, B. Viossat and A. Gautier, *Eur. J. Inorg. Chem.*, 2008, **2008**, 298-305.
33. T. L. Mindt, H. Struthers, L. Brans, T. Anguelov, C. Schweinsberg, V. Maes, D. Tourwé and R. Schibli, *J. Am. Chem. Soc.*, 2006, **128**, 15096-15097.
34. S. Warsink, R. M. Drost, M. Lutz, A. L. Spek and C. J. Elsevier, *Organometallics*, 2010, **29**, 3109-3116.
35. S. Gu, H. Xu, N. Zhang and W. Chen, *Chem. Asian J.*, 2010, **5**, 1677-1686.
36. K. Q. Vuong, M. G. Timerbulatova, M. B. Peterson, M. Bhadbhade and B. A. Messerle, *Dalton Trans.*, 2013, **42**, 14298-14308.
37. M. T. Zamora, M. J. Ferguson, R. McDonald and M. Cowie, *Organometallics*, 2012, **31**, 5463-5477.
38. S. N. Sluijter and C. J. Elsevier, *Organometallics*, 2014, **33**, 6389-6397.
39. Q. Zhao, M. Yu, L. Shi, S. Liu, C. Li, M. Shi, Z. Zhou, C. Huang and F. Li, *Organometallics*, 2010, **29**, 1085-1091.
40. Y. Zhou, J. Jia, W. Li, H. Fei and M. Zhou, *Chem. Commun.*, 2013, **49**, 3230-3232.
41. M. Chen, Y. Wu, Y. Liu, H. Yang, Q. Zhao and F. Li, *Biomaterials*, 2014, **35**, 8748-8755.
42. K. K.-W. Lo, *Acc. Chem. Res.*, 2015, **48**, 2985-2995.
43. L. Murphy, A. Congreve, L.-O. Pålsson and J. A. G. Williams, *Chem. Commun.*, 2010, **46**, 8743-8745.

44. Y. Liu, P. Zhang, X. Fang, G. Wu, S. Chen, Z. Zhang, H. Chao, W. Tan and L. Xu, *Dalton Trans.*, 2017, **46**, 4777-4785.
45. A. Sorvina, C. A. Bader, J. R. T. Darby, M. C. Lock, J. Y. Soo, I. R. D. Johnson, C. Caporale, N. H. Voelcker, S. Stagni, M. Massi, J. L. Morrison, S. E. Plush and D. A. Brooks, *Sci. Rep.*, 2018, **8**, 8191. View Article Online
DOI: 10.1039/C9DT01362H
46. F. Schibilla, A. Holthenrich, B. Song, A. L. Linard Matos, D. Grill, D. Rota Martir, V. Gerke, E. Zysman-Colman and B. J. Ravoo, *Chem. Sci.*, 2018, **9**, 7822-7828.
47. L. Hao, Z.-W. Li, D.-Y. Zhang, L. He, W. Liu, J. Yang, C.-P. Tan, L.-N. Ji and Z.-W. Mao, *Chem. Sci.*, 2019, **10**, 1285-1293.
48. Y. Chen, L. Qiao, L. Ji and H. Chao, *Biomaterials*, 2014, **35**, 2-13.
49. H. Huang, L. Yang, P. Zhang, K. Qiu, J. Huang, Y. Chen, J. Diao, J. Liu, L. Ji, J. Long and H. Chao, *Biomaterials*, 2016, **83**, 321-331.
50. Y. Li, B. Liu, X.-R. Lu, M.-F. Li, L.-N. Ji and Z.-W. Mao, *Dalton Trans.*, 2017, **46**, 11363-11371.
51. A. Mechler, B. D. Stringer, M. S. H. Mubin, E. H. Doeven, N. W. Phillips, J. Rudd-Schmidt and C. F. Hogan, *Biochim. Biophys. Acta Biomembr.*, 2014, **1838**, 2939-2946.
52. C. Yang, F. Mehmood, T. L. Lam, S. L.-F. Chan, Y. Wu, C.-S. Yeung, X. Guan, K. Li, C. Y.-S. Chung, C.-Y. Zhou, T. Zou and C.-M. Che, *Chem. Sci.*, 2016, **7**, 3123-3136.
53. G. J. Barbante, P. S. Francis, C. F. Hogan, P. R. Kheradmand, D. J. D. Wilson and P. J. Barnard, *Inorg. Chem.*, 2013, **52**, 7448-7459.
54. B. D. Stringer, L. M. Quan, P. J. Barnard, D. J. D. Wilson and C. F. Hogan, *Organometallics*, 2014, **33**, 4860-4872.
55. G. J. Barbante, E. H. Doeven, P. S. Francis, B. D. Stringer, C. F. Hogan, P. R. Kheradmand, D. J. D. Wilson and P. J. Barnard, *Dalton Trans.*, 2015, **44**, 8564-8576.
56. L. M. Quan, B. D. Stringer, M. A. Haghghatbin, J. Agugiaro, G. J. Barbante, D. J. D. Wilson, C. F. Hogan and P. J. Barnard, *Dalton Trans.*, 2019, **48**, 653-663.
57. C. Y. Chan, P. A. Pellegrini, I. Greguric and P. J. Barnard, *Inorg. Chem.*, 2014, **53**, 10862-10873.
58. C. Y. Chan, A. Noor, C. A. McLean, P. S. Donnelly and P. J. Barnard, *Chem. Commun.*, 2017, **53**, 2311-2314.
59. T. P. Pell, D. J. D. Wilson, B. W. Skelton, J. L. Dutton and P. J. Barnard, *Inorg. Chem.*, 2016, **55**, 6882-6891.
60. T. P. Pell, B. D. Stringer, C. Tubaro, C. F. Hogan, D. J. D. Wilson and P. J. Barnard, *Eur. J. Inorg. Chem.*, 2017, **2017**, 3661-3674.
61. T. L. Mindt, C. Müller, M. Melis, M. de Jong and R. Schibli, *Bioconjugate Chem.*, 2008, **19**, 1689-1695.
62. S. Hohloch, L. Suntrup and B. Sarkar, *Organometallics*, 2013, **32**, 7376-7385.
63. A. I. Poulain, D. Canseco-Gonzalez, R. Hynes-Roche, H. Müller-Bunz, O. Schuster, H. Stoeckli-Evans, A. Neels and M. Albrecht, *Organometallics*, 2011, **30**, 1021-1029.
64. G. A. Lamoureux, C., *Rev. Acc.*, 2009, **2009**, 251-264.
65. T. J. Siciliano, M. C. Deblock, K. M. Hindi, S. Durmus, M. J. Panzner, C. A. Tessier and W. J. Youngs, *J. Organomet. Chem.*, 2011, **696**, 1066-1071.
66. H. M. J. Wang and I. J. B. Lin, *Organometallics*, 1998, **17**, 972-975.
67. C. Kluba and T. Mindt, *Molecules*, 2013, **18**, 3206-3226.
68. C. B. Anderson, A. B. S. Elliott, J. E. M. Lewis, C. J. McAdam, K. C. Gordon and J. D. Crowley, *Dalton Trans.*, 2012, **41**, 14625-14632.
69. L. Brans, E. García-Garayoa, C. Schweinsberg, V. Maes, H. Struthers, R. Schibli and D. Tourwé, *Chem. Med. Chem.*, 2010, **5**, 1717-1725.
70. W. K. C. Lo, G. S. Huff, J. R. Cubanski, A. D. W. Kennedy, C. J. McAdam, D. A. McMorran, K. C. Gordon and J. D. Crowley, *Inorg. Chem.*, 2015, **54**, 1572-1587.
71. K. F. Donnelly, A. Petronilho and M. Albrecht, *Chem. Commun.*, 2013, **49**, 1145-1159.

72. A. B. Tamayo, B. D. Alleyne, P. I. Djurovich, S. Lamansky, I. Tsyba, N. N. Ho, R. Bau and M. E. Thompson, *J. Am. Chem. Soc.*, 2003, **125**, 7377-7387. View Article Online
DOI: 10.1039/C9DT01362H
73. J. C. Deaton and F. N. Castellano, in *Iridium(III) in Optoelectronic and Photonics Applications*, ed. E. Zysman-Coleman, Ed., John Wiley & Sons, Ltd, 2017, Chapter 1, pp. 1-69.
74. J. R. Lakowicz, *Principles of fluorescence spectroscopy*, Second edition. New York : Kluwer Academic/Plenum, 1999.
75. S. E. Laird and C. F. Hogan, in *Iridium(III) in Optoelectronic and Photonics Applications*, ed. E. Zysman-Colman, Ed., Wiley, 2017, vol. 2, pp. 359-414.
76. B. Liu, X. Liu, C. Chen, C. Chen and W. Chen, *Organometallics*, 2011, **31**, 282-288.
77. G. Sheldrick, *Acta Crystallogr., Sect. A*, 2008, **64**, 112-122.
78. O. V. Dolomanov, L. J. Bourhis, R. J. Gildea, J. A. K. Howard and H. Puschmann, *J. Appl. Crystallogr.*, 2009, **42**, 339-341.

Table of contents entry

Luminescent and electrochemiluminescent N-heterocyclic carbene-combined 1,2,3-triazole and 1,2,3-triazolylidene Ir(III) complexes have been prepared and their potential as luminescent probes in cell imaging has been evaluated.

